Clays and Clay Minerals, Vol. 51, No. 3, 301–308, 2003.

THE CRYSTAL STRUCTURE OF ROSCOELITE-1*M*

MARIA FRANCA BRIGATTI[1,*], ENRICO CAPRILLI[1], MARCO MARCHESINI[2] AND LUCIANO POPPI[1]

[1] Department of Earth Sciences, University of Modena and Reggio Emilia, Italy
[2] ENI-AGIP Towers, San Donato Milanese, Milano, Italy

Abstract—Single-crystal X-ray diffraction experiments were carried out on roscoelite crystals from Reppia, Val Graveglia, Italy. Roscoelite [structural formula: $^{XII}(Ba_{0.006}K_{0.994})^{IV}(Si_{3.150}Al_{0.850})^{VI}(Al_{0.040}Fe_{0.150}Mg_{0.100}Mn_{0.062}V_{1.696}Ti_{0.003})O_{10}(OH)_2$] shows a near-perfect three-dimensional stacking order with cell parameters a = 5.292(1), b = 9.131(2), c = 10.206(3) Å, β = 100.98(2)° and space group $C2/m$, which indicate a 1*M* polytype. The crystal structure was refined on the basis of F_o^2 for 846 unique reflections to $R1$ = 3.29% calculated using 746 unique observed reflections [$|F_o| \geqslant 4\sigma(F_o)$]. The mean tetrahedral cation–oxygen atom distance, $<T-O>$ = 1.641 Å, is close to the mean $<T-O>$ value obtained for dioctahedral true micas from the literature, whereas the octahedral sheet is characterized by a larger *cis*-octahedral cation–oxygen atom bond distance $<M2-O>$ = 2.020 Å which, together with the mean electron count, is consistent with V occupancy. The presence of V within the octahedral sheet produces the smallest tetrahedral rotation (α = 2.3°), the lowest flattening of the basal oxygen surface (Δz = 0.118 Å) and the narrowest interlayer separation (3.030 Å) in dioctahedral micas.

Key Words—Crystal Chemistry, Crystal Structure, Roscoelite, Vanadium Mica.

INTRODUCTION

The V-rich dioctahedral micas roscoelite, ideally $^{XII}K^{VI}(V_2^{3+}\square)^{IV}(AlSi_3)O_{10}(OH)_2$, and chernykhite, ideally $^{XII}Ba^{VI}(V_2^{3+}\square)^{IV}(Al_2Si_2)O_{10}(OH)_2$ (Rieder *et al.*, 1998), are relatively widespread in terrestrial rocks. Most of them occur in epithermal veins associated with Ag, Au and Pt deposits (*e.g.* Distler *et al.*, 2000; Kelley and Ludington, 2002; Ronacher *et al.*, 2002), from weakly metamorphosed sedimentary volcanogenic rocks (Rumyantseva, 1985), from the oxidized portions of sedimentary U-V ores (Breit, 1995; Ledeneva and Pakulnis, 1997), from black shales (Peacor *et al.*, 2000; Ankinovich *et al.*, 2001), and from reduction spots of continental and marine red beds (Hofmann, 1991; van Panhuys Sigler *et al.*, 1996). Roscoelite was found to be a 1*M* polytype (Gaines *et al.*, 1997) whereas chernykhite crystallizes either as $2M_1$ or $2M_2$ polytype with $C2/c$ or Cc space group symmetry (Kalinichenko *et al.*, 1974; Ankinovich *et al.*, 1997).

The aim of this work was to describe the crystal chemistry of a well crystallized roscoelite sample from Gambatesa mine (northern Italy) and to compare its structural features with a series of well characterized dioctahedral micas from the literature. To the best of our knowledge, this is the first accurate structural refinement of roscoelite-1*M*.

EXPERIMENTAL METHODS

The roscoelite sample was collected at the Gambatesa mine, near Reppia Village, val Graveglia, Genova (northern Italy). The roscoelite-bearing rock sample is very small (1.5 × 0.8 × 0.5 cm) and its mineral content very limited. Roscoelite is associated with manganaxinite, goldmanite, albite and Mn-Ca carbonates. The mineral occurs as flexible, dark-brown to black, platy pseudo-hexagonal crystals with a maximum dimension of 0.5 mm. A systematic description of minerals from val Graveglia, well known for the occurrence of Mn-rich minerals, can be found in Marchesini and Pagano (2001). Some new or unusual Mn- and V-bearing minerals have been discovered in this area. The genetic process accounting for these unusual phases has been related to hydrothermal events on sedimentary and ophiolitic rocks (Cabella *et al.*, 1991; Leoni *et al.*, 1996).

Several roscoelite crystals, optically homogeneous and inclusion-free, were hand picked from the bulk sample for single-crystal X-ray study. A thin, plate-shaped crystal displaying sharp reflections with little mosaic spread on precession photographs was chosen to determine cell dimension and to collect intensity data. Examination of zero and upper levels photographs indicated the extinction of reflections $h + k \neq 2n$, which define a *C*-centered cell. The cell geometry and the intensities of the diffraction pattern point to the space group $C2/m$, consistent with 1*M* polytype. The crystal was mounted on a Siemens P4P rotating-anode, fully automated, four-circle diffractometer operating at 50 kV and 140 mA with graphite-monochromatized MoKα radiation (λ = 0.71073 Å), equipped with the XSCANS software (Siemens, 1993).

Intensity data were collected up to 70°2θ. The intensities of the reflections hkl, $hk\bar{l}$, $h\bar{k}l$ and $h\bar{k}\bar{l}$ were measured using ω scan (ω scan widths 2.92°) and were corrected for absorption following the ψ-scan method of North *et al.* (1968). The values of the equivalent

* E-mail address of corresponding author:
brigatti@unimo.it
DOI: 10.1346/CCMN.2003.0510306

Table 1. Crystallographic data and refinement results for roscoelite.

a (Å)	5.292(1)	Radiation	MoKα
b (Å)	9.131(2)	$2\theta_{max}$(°)	70.0
c (Å)	10.206(3)	Observed reflections	2286
β (°)	100.98(2)	Unique reflections	846
V (Å^3)	484.1(2)	Data with $\|F_o\| \geq 4\sigma(F_o)$	746
Space group	*C*2/*m*	*R*1 (%)	3.29
Crystal size	0.14 × 0.12 × 0.07	wR^2 (%)	8.21
		R_{sym}	3.7
		GOF	0.913
		Extinction coefficient	9.62×10^{-3}

h, *k*, *l* ranges: −1 → 8, −14 → 14, −16 → 16

$$R1 = \frac{\sum ||F_o| - |F_c||}{\sum |F_o|} \times 100;\ wR^2 = \left[\frac{\sum w(F_o^2 - F_c^2)^2}{\sum (F_o^2)^2}\right]^{1/2};\ \text{GOF} = \left[\frac{\sum w(F_o^2 - F_c^2)^2}{n-p}\right]^{1/2}$$

$w = 1/[\sigma^2(F_o^2) + (0.556 \times P)^2 + 0.56 \times P]$, $P = (\max(F_o^2,0) + 2 \times F_c^2)/3$; *n* is the number of reflections and *p* is the number of parameters refined (actual refinement, $p = 55$).

monoclinic pairs were averaged and the resulting discrepancy factors R_{sym}, as well as other parameters relevant to data collection and structure refinement, are reported in Table 1. A set of over 40 reflections with both positive and negative 2θ angles was used to refine the unit-cell parameters (Table 1). Structure refinements based on F_o^2 were performed using the SHELXL-97 program (Sheldrick, 1997), in space group *C*2/*m*. The atomic scattering curves were taken from the *International Tables for X-ray Crystallography* (Ibers and Hamilton, 1974). Complete ionization of the cations at the *M*2 sites was adopted. The ionization states of Si and O atoms were considered as variables according to the linear combination of $xf(\text{Si}) + (1-x)\ f(\text{Si}^{4+})$ and $xf(\text{O}) + (1-x)\ f(\text{O}^{2-})$, *x* being variable.

Extinction correction was performed following Sheldrick (1997). All parameters were refined simultaneously, and no correlation >0.6 between site occupancies and thermal parameters was observed. The difference Fourier map did not show any significant residual electron density peaks, except for the existence of a small residual electron density close to the *M*2 site, which would indicate the presence of cations with ionic radii different from those of V. Unit-cell parameters, the number of total and unique reflections and the conventional discrepancy indices (*R* factors) are listed in Table 1. The final positional and displacement parameters are reported in Table 2. Table 3 lists selected interatomic distances and parameters obtained from structure refinement. Observed and calculated structure factors are available from the author.

Chemical composition (Table 4) was obtained on the same crystal as used for X-ray data collection with a wavelength-dispersion ARL-SEMQ electron microprobe (operating conditions: 15 kV accelerating voltage, 15 nA sample current, and spot size ~8 μm). Analyses and data reductions were performed using the Probe software package by Donovan (1995). The following standards were employed for the determination of roscoelite composition: microcline (K), albite (Na), spessartine (Al, Mn), ilmenite (Fe), clinopyroxene (Si), olivine (Mg), and vanadinite (V). No systematic compositional variations were observed in the crystal. The F and Cl are both below the detection limit. The cation content obtained, based on cations and on $O_{10}(OH)_2$ anions, was distributed by combining the results of structure refinement and electron probe analysis.

Table 2. Atomic coordinates, equivalent isotropic and anisotropic displacement parameters (Å$^2 \times 10^3$) for roscoelite.

Atom	*x*/*a*	*y*/*b*	*z*/*c*	U_{eq}	U_{11}	U_{22}	U_{33}	U_{23}	U_{13}	U_{12}
O1	0.0471(5)	0	0.1727(2)	20(1)	26(1)	14(1)	17(1)	0	−1(1)	0
O2	0.3125(3)	0.2449(2)	0.1609(2)	19(1)	15(1)	26(1)	15(1)	−1(1)	1(1)	−8(1)
O3	0.1416(3)	0.1825(1)	0.3880(2)	14(1)	12(1)	16(1)	12(1)	0(1)	2(1)	−1(1)
O4	0.1029(4)	0.5	0.3924(2)	18(1)	15(1)	23(1)	18(1)	0	7(1)	0
T	0.0805(1)	0.1695(1)	0.2254(1)	8(1)	6(1)	9(1)	10(1)	0(1)	1(1)	0(1)
*M*1	0	0	0.5	8(3)						
*M*2	0	0.3350(1)	0.5	11(1)	8(1)	11(1)	14(1)	0	−1(1)	0
A	0	0.5	0	29(1)	27(1)	28(1)	30(1)	0	4(1)	0

U_{eq} is defined as one third of the trace of the orthogonalized U_{ij} tensor. The anisotropic displacement factor exponent takes the form: $\exp\{-2\pi^2[h^2\ (a^*)^2 U_{11} + ... + 2hka^*b^*U_{12} + ...]\}$.

https://doi.org/10.1346/CCMN.2003.0510306 Published online by Cambridge University Press

Table 3. Selected bond lengths (Å) and parameters derived from structure refinement of roscoelite.

Tetrahedral			
T–O1	1.6373(9)	<O–O>$_{basal}$ (Å)	2.645
T–O2	1.643(2)	α (°)	2.3
T–O2′	1.649(2)	Δ*z* (Å)	0.118
T–O3	1.634(2)	τ (°)	111.7
<*T*–O>	1.641	TAV (°^{2})	6.8
		Volume (Å^3)	2.26
		Thickness (Å)	2.251
Octahedral			
*M*1–O3 (×4)	2.230(2)	ψ_{M1}(°)	60.0
*M*1–O4 (×2)	2.178(3)	ψ_{M2} (°)	56.8
<*M*1–O>	2.213	OAV$_{M1}$	55.6
*M*2–O3 (×2)	2.026(2)	OAV$_{M2}$	24.9
*M*2–O3′ (×2)	2.033(2)	Volume$_{M1}$ (Å^3)	14.07
*M*2–O4 (×2)	2.000(2)	Volume$_{M2}$ (Å^3)	10.87
<*M*2–O>	2.020	Thickness (Å)	2.215
Interlayer			
K–O1 (×2)	3.089(2)	<K–O>$_{inner}$	3.063
K–O1′ (×2)	3.234(3)	<K–O>$_{outer}$	3.167
K–O2 (×4)	3.050(2)	Δ(*K*–O) (Å)	0.104
K–O2′ (×4)	3.134(2)	Thickness (Å)	3.030
K–O4 (×2)	3.938(2)		

α (tetrahedral rotation angle) = $\sum_{i=1}^{6}\alpha_i/6$ where $\alpha_i = |120° - \phi_i|/2$ and where ϕ_i is the angle between basal edges of neighboring tetrahedra articulated in the ring

$\Delta z = [Z_{(O_{basal})max} - Z_{(O_{basal})min}]$ [*c*sinβ]

τ (tetrahedral flattening angle) = $\sum_{i=1}^{3}(O_{basal} - \hat{T} - O_{basal})/3$

TAV (tetrahedral angle variance) = $\sum_{i=1}^{3}(\theta_i - 109.47°)^2/5$ (Robinson *et al.* (1971)

ψ (octahedral flattening angle) = cos^{-1}[octahedral thickness/(2<*M*–O>)] (Donnay *et al.* (1964)

OAV (octahedral angle variance) = $\sum_{i=1}^{12}(\theta_i - 90°)^2/11$ (Robinson *et al.* (1971).

CRYSTAL CHEMISTRY OF ROSCOELITE

The unusual V-rich composition of roscoelite, $^{XII}(Ba_{0.006}K_{0.994})^{IV}(Si_{3.150}Al_{0.850})^{VI}(Al_{0.040}Fe_{0.150}Mg_{0.100}Mn_{0.062}V_{1.696}Ti_{0.003})O_{10}(OH)_2$, results in a different structural arrangement when compared with other dioctahedral micas. Dioctahedral micas are usually characterized by $2M_1$ and, more rarely, by 3*T* polytype. Only a limited number of dioctahedral micas have been refined in the 1*M* polytype (Sidorenko *et al.*, 1977; Soboleva *et al.*, 1977; Zhoukhlistov *et al.*, 1977), but to *R* values always >10%. Roscoelite, like many other dioctahedral micas, is characterized by a small *trans*-octahedral site (*M*1) occupancy. The *M*1 mean electron count was refined to be 1. The *cis*-octahedral site (*M*2) mean electron count is consistent with V occupancy, with limited substitutions from other cations, which is consistent with chemical data.

The main structural differences between roscoelite and other K-rich dioctahedral micas affect the octahedral site. The mean <*M*2–O> distance was refined to be 2.020 Å, a larger value than usual for muscovite (<*M*2–O> = 1.916 Å for muscovite according to Guggenheim *et al.* (1987)). This difference can be ascribed to the larger size of V compared with Al (Shannon, 1976). The mean <*M*1–O> distance does not differ significantly from the mean value commonly found for muscovite crystals. The difference between the <*M*1–O> and <*M*2–O> distances for roscoelite is significantly less than in other dioctahedral micas. In dioctahedral micas, the *M*1 site is larger than the *M*2 site and the octahedral flattening angle for *M*1 is greater than for *M*2 as well. Figure 1a illustrates the relationship between Δ<*M*–O> (<*M*1–O> – <*M*2–O>) and $\Delta\psi(\psi_{M1}-\psi_{M2})$. A good correlation between these structural parameters is expected as they are not fully independent of one another. However the influence of Al substitutions on octahedral topology can be clearly observed. As Al in *M*2 sites is increasingly substituted by larger cations (see, for example, celadonitic muscovite, celadonite and chromphyllite), the difference in size between octahedral distances decreases as well as their distortion.

This mechanism produces an expansion of the octahedral lateral dimension. As the distortion of the octahedral sheet decreases, its lateral dimension, measured by $a \times b$, increases (Figure 1b). The increase in the octahedral lateral dimension is correlated with an increase in octahedral thickness, as shown in Figure 2.

https://doi.org/10.1346/CCMN.2003.0510306 Published online by Cambridge University Press

Table 4. Chemical composition (oxide wt.%), chemical formula (a.p.f.u.), refined (*X*ref) and calculated (EPMA) site-occupancy (e.p.f.u.) for octahedral (*M*) and interlayer (K) sites of roscoelite.

Oxide (wt.%)		Chemical formula (a.p.f.u.) based on $O_{10}OH_2$	
SiO_2	42.32	^{IV}Si	3.150
Al_2O_3	10.14	^{IV}Al	0.850
TiO_2	0.05	^{IV}Sum	4.000
V_2O_3	28.42	^{VI}Al	0.040
FeO	2.42	$^{VI}V^{3+}$	1.696
MgO	0.91	$^{VI}Fe^{2+}$	0.150
MnO	0.02	^{VI}Mg	0.100
MnO	0.98	^{VI}Mn	0.062
BaO	0.23	^{VI}Ti	0.003
K_2O	10.47	^{VI}Sum	2.051
H_2O	4.02	^{XII}Ba	0.006
		^{XII}K	0.994
Sum	99.98	^{XII}Sum	1.000
Refined and calculated site occupancy (e.p.f.u.)			
$M1_{Xref}$	1.25	K_{Xref}	19.05
$M2_{Xref}$	22.41	K_{EPMA}	19.22
$(M1 + 2\times M2)_{Xref}$	46.07		
$(M1 + 2\times M2)_{EPMA}$	46.27		

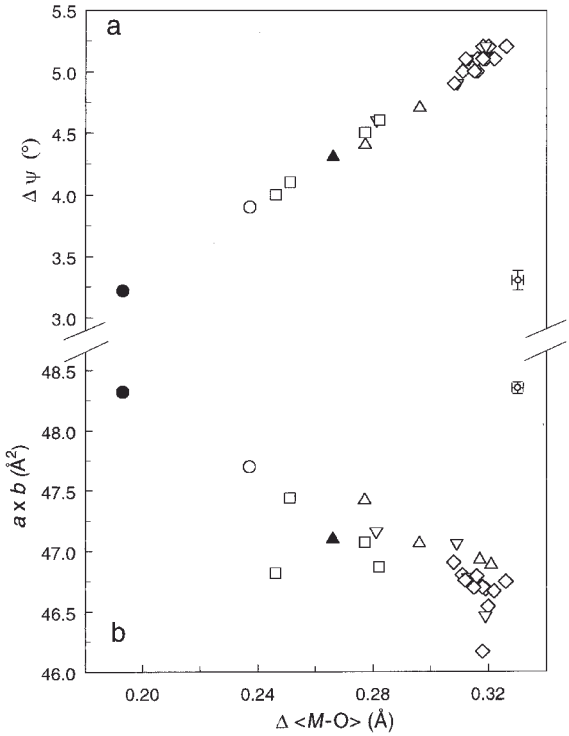

Figure 1. (a) Relationship between $\Delta\psi(\psi_{M1}-\psi_{M2})$ (°) and Δ<*M*–O> (<*M*1–O>–<*M*2–O>) (Å); (b) relationships between unit-cell area ($a\times b$) (Å^2), measured on (001), and Δ<*M*–O>. Symbols and samples: filled circle = roscoelite, this study; open circle = chromphyllite (Evsyunin *et al.*, 1997); filled triangle = celadonite (Güven, 1971); open square = Li-containing muscovite (Brigatti *et al.*, 2001b); open inverted triangle = Cr-containing celadonitic muscovite (Rule and Bailey, 1985) and Cr-containing muscovite (Brigatti *et al.*, 2001a); open triangle = celadonitic muscovite (Brigatti *et al.*, 1998a; Knurr and Bailey, 1986); diamond = muscovite (Brigatti *et al.*, 1998a; Rothbauer, 1971; Gugghenheim *et al.*, 1987; Catti *et al.*, 1989). The estimated standard deviation of mean value is reported on the right of each plot.

Unlike trioctahedral micas (Brigatti *et al.*, 2003), both lateral dimensions and the thickness of the octahedral sheet are strongly affected by octahedral substitutions.

The unusual octahedral topology in roscoelite accounts for the difference in the flattening of the tetrahedral basal oxygen plane (Δz) and for the distortion of the tetrahedral ring from hexagonal symmetry (α), when compared to other dioctahedral micas. In particular, as demonstrated by Lee and Guggenheim (1981), a small dimensional misfit between the *M*1 and *M*2 sites (estimated by Δ<*M*–O>), produces a slight corrugation of the basal oxygen plane (estimated by Δz) and *vice versa*. Δz in roscoelite was calculated to be 0.118 Å, whereas the value determined for muscovite is 0.213 Å (Guggenheim *et al.*, 1987; muscovite sample from Panasqueira) and for chromphyllite, the Cr^{3+}-rich dioctahedral mica, is 0.158 Å (Evsyunin *et al.*, 1997).

The tetrahedral rotation angle was computed to be 2.3° for roscoelite, whereas the average for other dioctahedral true micas considered is 10.2°. This feature can be accounted for considering that:

$$\alpha = \cos^{-1}\left(\frac{\sqrt{3}}{2}\cdot\frac{\langle O3 - O3\rangle}{^{[IV]}\langle O - O\rangle_{basal}}\right)$$

(Brigatti and Guggenheim, 2002)

Accordingly, an increase in <O3–O3>, associated with an increase in the octahedral sheet lateral dimensions, produces a decrease in α. Interlayer topology is different for roscoelite and other dioctahedral micas, mainly due to the influence of α over interlayer cation coordination.

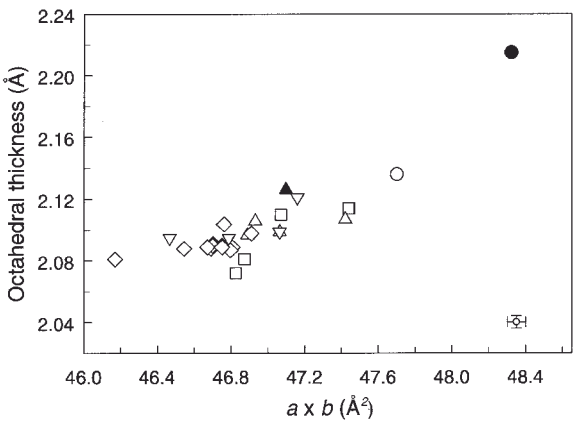

Figure 2. Relationship between octahedral thickness (Å) and unit-cell area ($a\times b$) (Å^2), measured on (001). Symbols and samples as in Figure 1. The estimated standard deviation of mean value is reported on the bottom (right corner) of the plot.

https://doi.org/10.1346/CCMN.2003.0510306 Published online by Cambridge University Press

In trioctahedral micas, the *M*1 site was found to be mostly affected by octahedral chemical composition, irrespective of the actual occupancy of the octahedral cation: the *M*1 site is more sensitive than *M*2 sites to chemical substitutions, irrespective of the actual distribution of substituting cations between octahedral sites (Brigatti *et al.*, 2003). A structural modification involving *M*1 site size does not affect the layer dimensions as much as a variation in *M*2 site size, given the 2:1 ratio between *M*2 and *M*1 occurring in 1*M* polytype with *C*2/*m* symmetry. The same ratio applies to $2M_1$ polytype (*C*2/*c* symmetry), characterizing most dioctahedral micas. Following the vacant *M*1 site, in dioctahedral micas, including roscoelite, octahedral chemical composition and, in particular, the dimensions of the octahedral cations, mostly affect *M*2 site dimensions. Figure 3a shows the dependence of the <*M*2–O> bond lengths on the average octahedral cation ionic radius, $\langle r_M \rangle$ (Shannon, 1976), as estimated by chemical composition. A plot of the unit-cell parameter, *a vs.* $\langle r_M \rangle$ is also reported to confirm the strong influence of *M*2 site dimensions over the whole layer (Figure 3b). Octahedral chemical composition appears to be the predominant chemical factor affecting α, as demonstrated in Figure 3c. In this way the octahedral chemical composition affects the topology of the tetrahedral sheet as well.

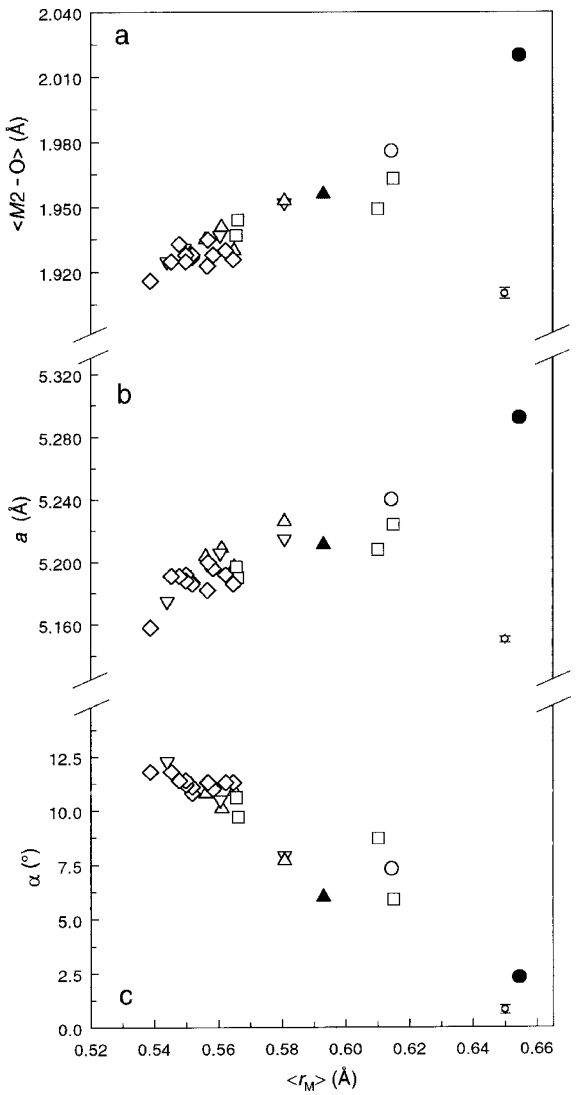

Figure 3. Variation of (a) <*M*2–O> (Å) bond lengths; (b) unit-cell parameter *a* (Å); and (c) tetrahedral α(°) with mean octahedral ionic radius (Å) (Shannon, 1976). Symbols and samples as in Figure 1. The estimated standard deviation of mean value is reported in the bottom (right corner) of the plots.

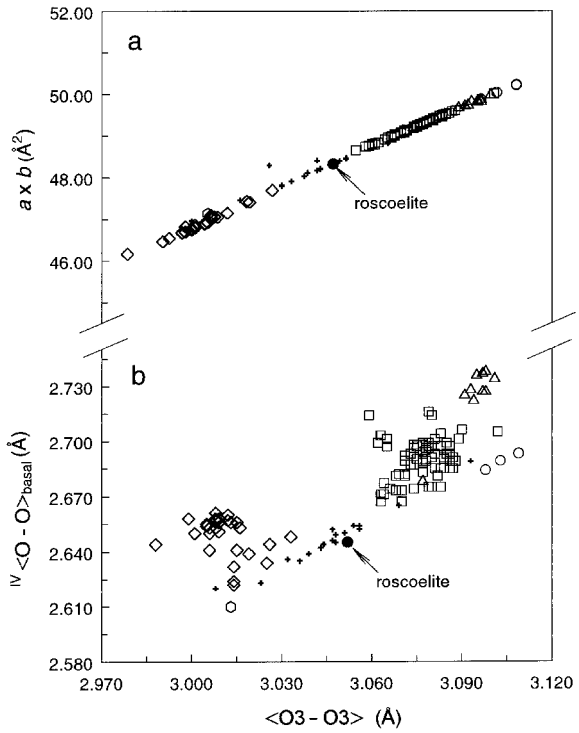

Figure 4. (a) Variation between unit-cell area ($a \times b$) (Å^2), measured on (001), and (b) mean basal tetrahedral edge (^{IV}<O–O>$_{basal}$) (Å) with the mean value of octahedral <O3–O3> (Å) edge for dioctahedral and trioctahedral micas. Symbols: filled circle = roscoelite, this study; open symbols = samples from the literature: circle = annite; square = phlogopite, ferroan plogopite, and magnesian annite; cross = polylithionite, ferroan polylithionite and siderophyllite, diamond = muscovite, celedonitic muscovite, Li- and Cr-containing muscovite; triangle = tetra-ferriphlogopite; hexagon = norrishite. Samples from the literature are from: Takeda and Donnay (1966); Rothbauer (1971); Joswig (1972); Hazen and Burnham (1973); McCauley *et al.* (1973); Takeda and Morosin (1975); Takeda and Ross (1975); Guggenheim and Bailey (1977); Semenova *et al.* (1977); Kato *et al.* (1979); Bohlen *et al.* (1980); Guggenheim (1981); Hazen *et al.* (1981); Otha *et al.* (1982); Backhaus (1983); Guggenheim and Kato (1984); Rule and Bailey (1985); Guggenheim *et al.* (1987); Catti *et al.* (1989); Brigatti and Davoli (1990); Brigatti *et al.* (1991); Bigi *et al.* (1993); Brigatti and Poppi (1993); Weiss *et al.* (1993); Amisano-Canesi *et al.* (1994); Bigi and Brigatti (1994); Alietti *et al.* (1995); Brigatti *et al.* (1996, 1998b, 1999); Hawthorne *et al.* (1999); Russell and Guggenheim (1999); Brigatti *et al.* (2000a,b, 2001a,b).

https://doi.org/10.1346/CCMN.2003.0510306 Published online by Cambridge University Press

The 1*M* polytype is very uncommon for dioctahedral micas. However, the low *R* values resulting from refinement in *C*2/*m* symmetry suggest that the assumed space group is correct and consistent with 1*M* polytype as well as with disorder between *cis*-site occupancies. The unusual layer stacking for this dioctahedral mica can be ascribed to the small size difference between the *M*1 and *M*2 sites, resulting in a topological arrangement close to that of trioctahedral micas. Figure 4a shows that dioctahedral micas have a smaller unit-cell area and <O3–O3> length than trioctahedral micas. Roscoelite, like trioctahedral Li-rich micas, is intermediate. Figure 4b shows that a poor correlation exists in dioctahedral $2M_1$ micas between tetrahedral and octahedral distances, whereas there is a good correlation for trioctahedral micas. Roscoelite follows the trend typical of trioctahedral micas and plots close to Li-rich trioctahedral micas.

CONCLUSIONS

Roscoelite follows some trends common to dioctahedral micas, such as the influence of octahedral chemical composition on the *M*2 site, and some others common to trioctahedral micas, *e.g.* the correlation between tetrahedral and octahedral distances on (001) and the polytypic arrangement.

ACKNOWLEDGMENTS

The authors are grateful to M.D. Welch and to an anonymous referee for their constructive reviews. D.C. Bain and P.J. Heaney are thanked for their editorial handling of the manuscript. This work was supported financially by MURST and by CNR of Italy.

REFERENCES

Alietti, E., Brigatti, M.F. and Poppi, L. (1995) The crystal structure and chemistry of high-aluminium phologopite. *Mineralogical Magazine*, **59**, 149–157.

Amisano-Canesi, A., Chiari, G., Ferraris, G., Ivaldi, G. and Soboleva, S.V. (1994) Muscovite- and phengite-3*T*: crystal structure and conditions of formation. *European Journal of Mineralogy*, **6**, 489–496.

Ankinovich, E.A., Bekenova, G.K., Kompaneitsev, V.P., Kotel'nikov, P.E. and Savostin, B.A. (1997) Vanadium and vanadium-bearing micas from the Cambrian carbonaceous-siliceous sedimentary rocks in the Greater Karatau Range of southern Kazakhstan. Part I. Chernykhites, Roscoelites. *Geologiya Kazakhstana*, **4**, 84–93 (abstract).

Ankinovich, E.A., Bekenova, G.K., Kompaneitsev, V.P., Kotel'nikov, P.E. and Savostin, B.A. (2001) Vanadium and vanadium-bearing micas from the Cambrian carbon-siliceous formation of the Bolskoi Karatau Range (south Kazakhstan). Part 2. V^{4+}-Ba-phengites. Vanadium bearing muscovite and phengites. *Geologiya Kazakhstana*, **2**, 13–23 (abstract).

Backhaus, K.O. (1983) Structure refinement of a lepidolite-1M. *Crystal Research Technology*, **18**, 1253–1260.

Bigi, S. and Brigatti, M.F. (1994) Crystal chemistry and microstructures of plutonic biotite. *American Mineralogist*, **79**, 63–72.

Bigi, S., Brigatti, M.F., Mazzucchelli, M. and Rivalenti, G. (1993) Crystal chemical variations in Ba-rich biotites from gabbroic rocks of lower crust (Ivrea Zone, NW Italy). *Contributions to Mineralogy and Petrology*, **113**, 87–99.

Bohlen, S.R., Peacor, D.R. and Essene, E.J. (1980) Crystal chemistry of a metamorphic biotite and its significance in water barometry. *American Mineralogist*, **65**, 55–62.

Breit, G.N. (1995) Origin of clay minerals associated with V-U deposits in the Entrada Sandstone, Placerville Mining District, Southwestern Colorado. *Economic Geology*, **90**, 407–429.

Brigatti, M.F. and Davoli, P. (1990) Crystal structure refinement of 1*M* plutonic biotites. *American Mineralogist*, **75**, 305–313.

Brigatti, M.F. and Guggenheim S. (2002) Mica crystal chemistry and the influence of pressure, temperature, and solid solution on atomistic models. Pp. 1–100 in: *Micas: Crystal Chemistry & Metamorphic Petrology* (A. Mottana, F. P. Sassi, J. B. Thompson, Jr. and S. Guggenheim, editors). Reviews in Mineralogy and Geochemistry, **46**. Mineralogical Society of America, Washington, D.C.

Brigatti, M.F. and Poppi, L. (1993) Crystal chemistry of Ba-rich trioctahedral micas-1M. *European Journal of Mineralogy,* **5**, 857–871.

Brigatti, M.F., Galli, E. and Poppi, L. (1991) Effect of Ti substitution in biotite-1*M* crystal chemistry. *American Mineralogist,* **76**,1174–1183.

Brigatti, M.F., Medici, L., Saccani, E. and Vaccaro, C. (1996) Crystal chemistry and petrologic significance of Fe^{3+}-rich phlogopite from the Tapira carbonatite complex, Brazil. *American Mineralogist,* **81**, 913–927.

Brigatti, M.F., Frigieri, P. and Poppi, L. (1998a) Crystal chemistry of Mg-, Fe-bearing muscovites-$2M_1$. *American Mineralogist*, **83**, 775–785.

Brigatti, M.F., Lugli, C., Poppi, L. and Elburg, M. (1998b) Crystal chemistry of biotites from mafic enclaves in the Warburton granodiorite, Lachlan Fold Belt (Australia). *European Journal of Mineralogy,* **10**, 855–864.

Brigatti, M.F., Lalonde, A.E. and Medici, L. (1999) Crystal chemistry of $^{IV}Fe^{3+}$-rich phlogopites: a combined single-crystal X-ray and Mössbauer study. Pp. 317–327 in: *Clays for Our Future: Proceedings of the 11th International Clay Conference, Ottawa, Canada, 1997* (H. Kodama, A. Mermut, and J.K. Torrance, editors).

Brigatti, M.F., Frigieri, P., Ghezzo, C. and Poppi, L. (2000a) Crystal chemistry of Al-rich biotites coexisting with muscovites in peraluminous granites. *American Mineralogist*, **85**, 436–448.

Brigatti, M.F., Lugli, C., Poppi, L., Foord, E.E. and Kile, D.E. (2000b) Crystal chemical variations in Li- and Fe-rich micas from Pikes Peak Batholith (central Colorado). *American Mineralogist,* **85**, 1275–1286.

Brigatti, M.F., Galli, E., Medici, L., Poppi, L., Cibin, G., Marcelli, A. and Mottana, A. (2001a) Crystal structure refinement and X-ray absorption spectroscopy of chromium-containing muscovite. *European Journal of Mineralogy*, **13**, 377–390.

Brigatti, M.F., Kile, D.E. and Poppi, M. (2001b) Crystal structure and crystal chemistry of lithium-bearing muscovite-$2M_1$. *The Canadian Mineralogist*, **39**, 1171–1180.

Brigatti, M.F., Guggenheim S. and Poppi, M. (2003) Crystal chemistry of the 1*M* mica polytype: the octahedral sheet. *American Mineralogist*, **88**, 667–675.

Cabella, R., Gaggero, L. and Lucchetti, G. (1991) Isothermal-isobaric mineral equilibria in braunite-, rhodonite-, johannsenite-, calcite-bearing assemblages from Northern Appennine metacherts (Italy). *Lithos*, **27**, 149–154.

Catti, M., Ferraris, G. and Ivaldi, G. (1989) Thermal strain analysis in the crystal structure of muscovite at 700ºC.

European Journal of Mineralogy, **1**, 625–632.
Distler, V.V., Yudovskaya, M.A., Prokof'ev, V.A., Sluzhenikin, S.F., Mokhov, A.V. and Mun, Ya.V. (2000) Hydrothermal platinum mineralization in the Waterberg deposit (Transvaal, South Africa). *Geologiya Rudnykh Mestorozhdenii*, **42**, 363–376 (abstact).
Donnay, G., Morimoto, N., Takeda, H. and Donnay, J.D.H. (1964) Trioctahedral one-layer micas: I. Crystal structure of a synthetic iron mica. *Acta Crystallographica*, **17**, 1369–1373.
Donovan, J.J. (1995) *PROBE: PC-based data acquisition and processing for electron microprobes*. Advanced Microbeam, 4217 King Graves Rd., Vienna, Ohio, 44473.
Evsyunin, V.G., Kashaev, A.A. and Rastsvetaeva, R.K. (1997) Crystal structure of a new representative of Cr micas. *Crystallography Reports*, **42**, 571–574.
Gaines, R.V., Skinner, H.C., Foord, E.E., Mason, B. and Rosenzweig, A. (1997) *Dana's new mineralogy: the system of mineralogy of James Dwight Dana and Edward Salisbury Dana*, 8th edition. Wiley, Chichester, UK.
Guggenheim, S. (1981) Cation ordering in lepidolite. *American Mineralogist,* **66**,1221–1232.
Guggenheim, S. and Bailey, S.W. (1977) The refinement of zinnwaldite-1*M* in subgroup symmetry. *American Mineralogist,* **62**, 1158–1167.
Guggenheim, S. and Kato, T. (1984) Kinoshitalite and Mn phlogopites: Trial refinements in subgroup symmetry and further refinement in ideal symmetry. *Mineralogical Journal*, **12**, 1–5.
Guggenheim, S., Chang, Y.-H. and Koster van Groos, A.F. (1987) Muscovite dehydroxylation: High-temperature studies. *American Mineralogist,* **72**, 537–550.
Güven, N. (1971) The crystal structures of $2M_1$ phengite and $2M_1$ muscovite. *Zeitschift für Kristallographie*, **134**, 196–212.
Hawthorne, F.C., Teertstra, D.K. and Černý, P. (1999) Crystal-structure refinement of a rubidian cesian phlogopite. *American Mineralogist,* **84**, 778–781.
Hazen, R.M. and Burnham, C.W. (1973) The crystal structures of one-layer phlogopite and annite. *American Mineralogist,* **58**, 889–900.
Hazen, R.M., Finger, L.W. and Velde, D. (1981) Crystal structure of a silica- and alkali-rich trioctahedral mica. *American Mineralogist,* **66**, 586–591.
Hofmann, B.A. (1991) Mineralogy and geochemistry of reduction spheroids in red beds. *Mineralogy and Petrology*, **44**, 107–124.
Ibers, J.A. and Hamilton, W.C. (1974) *International Tables for X-ray Crystallography*, vol. **4**. Kynoch Press, Birmingan, UK, 99–101.
Joswig, W. (1972) Neutronenbeugungsmessungen an einem 1*M*-phlogopit. *Neues Jahrbuch für Mineralogie Monatshefte,* 1–11.
Kalinichenko, A.M., Matyash, I.V., Rozhdestvenskaya, I.V. and Frank-Kamenetskii, V.A (1974) Refinement of the structural characteristics of chernykhite from proton magnetic resonance data. *Kristallografiya,* **19**, 123–125.
Kato, T., Miúra, Y., Yoshii, M. and Maeda, K. (1979) The crystal structure of 1*M*-kinoshitalite, a new barium brittle mica and 1*M*-manganese trioctahedral micas. *Mineralogical Journal*, **9**, 392–408.
Kelley, K.D. and Ludington, S. (2002) Cripple Creek and other alkaline-related gold deposits in the southern Rocky Mountains, USA: influence of regional tectonics. *Mineralium Deposita*, **37**, 38–60.
Knurr, R.A. and Bailey, S.W. (1986) Refinement of Mn-substituted muscovite and phlogopite. *Clays and Clay Minerals*, **34**, 7–16.
Ledeneva, N.V. and Pakulnis, G.V. (1997) Mineralogy and formation conditions of uranium-vanadium deposits in the Onega basin (Russia). *Geology of Ore Deposits*, **39**, 219–228.
Lee, J.H. and Guggenheim, S. (1981) Single crystal X-ray refinement of pyrophyllite-1*Tc*. *American Mineralogist,* **66**, 350–357.
Leoni, L., Marroni, M., Sartori, F. and Tamponi, M. (1996) Metamorphic grade in metapelites of the Internal Liguride Units (Northern Apennines, Italy). *European Journal of Mineralogy*, **8**, 35–50.
Marchesini, M. and Pagano, R. (2001) The Val Graveglia manganese district, Liguria, Italy. *The Mineralogical Record*, **32**, 349–415.
McCauley, J.W., Newnham, R.E. and Gibbs, G.V. (1973) Crystal structure analysis of synthetic fluorophlogopite. *American Mineralogist,* **58**, 249–254.
North, A.C.T., Phillips, D.C. and Mathews, F.S. (1968) A semi-empirical method of absorption correction. *Acta Crystallographica*, **A24**, 351–359.
Ohta, T., Takeda, H. and Takéuchi, Y. (1982) Mica polytypism: similarities in the crystal structures of coexisting 1*M* and $2M_1$ oxybiotite. *American Mineralogist,* **67**, 298–310.
Peacor, D.R., Coveney, R.M. and Zhao, G.M. (2000) Authigenic illite and organic matter: The principal hosts of vanadium in the Mecca Quarry Shale at Velpen, Indiana. *Clays and Clay Minerals*, **48**, 311–316.
Rieder, M., Cavazzini, G., D'yakonov, Y.S., Frank-Kamenetskii, V.A., Gottardi, G., Guggenheim, S., Koval, P.V., Müller, G., Neiva, A.M.R., Radoslovich, E.W., Robert, J.-L., Sassi, F.P., Takeda, H., Weiss, Z. and Wones, D.R. (1998) Nomenclature of the micas. *Clays and Clay Minerals*, **46**, 586–595.
Robinson, K., Gibbs, G.V. and Ribbe, P.H. (1971) Quadratic elongation: a quantitative measure of distortion in coordination polyhedra. *Science,* **172**, 567–570.
Ronacher, E., Richards, J.P., Villeneuve, M.E. and Johnston, M.D. (2002) Short life-span of the ore-forming system at the Porgera gold deposit, Papua New Guinea: laser 40Ar/39Ar dates for roscoelite, biotite, and hornblende. *Mineralium Deposita,* **37,** 75–86.
Rothbauer, von, R. (1971) Untersuchung eines $2M_1$-Muskovits mit Neutronenstrahlen. *Neues Jahrbuch für Mineralogie Monatshefte,* 143–154.
Rule, A.C. and Bailey, S.W. (1985) Refinement of the crystal structure of phengite-$2M_1$. *Clays and Clay Minerals*, **33**, 403–409.
Rumyantseva, E.V. (1985) Some minerals of chromium-vanadium glimmerites of Karelia. *Zapiski Vsesoyuznogo Mineralogicheskogo Obshchetsva*, **114**, 55–62 (abstract).
Russell, R.L. and Guggenheim, S. (1999) Crystal structures of hydroxyphlogopite at high temperatures and heat-treated biotites: The influence of the O,OH,F site. *The Canadian Mineralogist*, **37**, 711–720.
Semenova, T.F., Rozhdestvenskaya, I.V. and Frank-Kamenetskii, V.A. (1977) Refinement of the crystal structure of tetraferriphlogopite. *Soviet Physics-Crystallography*, **22**, 680–683.
Shannon, R.D. (1976) Revised effective ionic radii and systematic studies of interatomic distances in halides and chalcogenides. *Acta Crystallographica A***, 32**, 751–767.
Sheldrick, G.M. (1997) *SHELX-97, a program for crystal structure refinement*. University of Göttingen, Germany.
Sidorenko, O.V., Zvyagin, B.B. and Soboleva, S.V. (1977) Crystal structure of 3T paragonite. *Soviet Physics-Crystallography*, **22**, 557–559.
Siemens (1993) *XSCANS: X-ray single crystal analysis system – Technical reference*. Siemens instruments, Madison, Wisconsin, USA.
Soboleva, S.V., Sidorenko, O.V. and Zvyagin, B.B. (1977)

Crystal structure of paragonite 1*M*. *Soviet Physics-Crystallography,* **22**, 291–294.

Takeda, H. and Donnay, J.D.H. (1966) Trioctahedral one-layer micas. III. Crystal structure of a synthetic lithium fluormica. *Acta Crystallographica*, **20**, 638–646.

Takeda, H. and Morosin, B. (1975) Comparison of observed and predicted structural parameters of mica at high temperature. *Acta Crystallographica*, **B31**, 2444–2452.

Takeda, H. and Ross, M. (1975) Mica polytypism: Dissimilarities in the crystal structures of coexisting 1M and 2M1 biotite. *American Mineralogist,* **60**,1030–1040.

van Panhuys Sigler, M., Trewin, N.H. and Still, J. (1996) Roscoelite associated with reduction spots in Devonian red beds, Gamrie Bay, Banffshire. *Scottish Journal of Geology*, **32**, 127–132.

Weiss, Z., Rieder, M., Smrčok, L., Petríček, V. and Bailey, S.W. (1993) Refinement of the crystal structures of two "protolithionites". *European Journal of Mineralogy,* **5**, 493–502.

Zhoukhlistov, A.P., Zvyagin, B.B., Lazarenko, E.K. and Pavlishin, V.I. (1977) Refinement of the crystal structure of ferrous seladonite. *Soviet Physics-Crystallography*, **22**, 284–288.

(*Received 10 September 2002; revised 7 January 2003; Ms. 714*)